

## Catalysis

# Kinetics and Mechanism of the Racemization of Aryl Allenes Catalyzed by Cationic Gold(I) Phosphine Complexes

Robert J. Harris, Kohki Nakafuku, and Ross A. Widenhoefer\*<sup>[a]</sup>

**Abstract:** The kinetics of the racemization of aromatic 1,3-disubstituted allenes catalyzed by gold phosphine complexes has been investigated. The rate of gold-catalyzed allene racemization displayed first-order dependence on allene, and catalyst concentration and kinetic analysis of gold-catalyzed allene racemization as a function of allene and phosphine electron-donor ability established the accumulation of electron density on the phosphine atom and the depletion of electron density on the terminal allenyl carbon atoms in the rate-limiting transition state for racemi-

zation. These and other observations were in accord with a mechanism for allene racemization involving rapid and reversible inter- and intramolecular allene exchange followed by turnover-limiting, unimolecular conversion of a chiral gold  $\eta^2$ -allene complex to an achiral  $\eta^1$ -allylic cation intermediate through a bent and twisted  $\eta^1$ -allene transition state. With respect to proper ligand selection, these studies reveal that both electron-poor phosphine ligands and polar solvents facilitate racemization.

## Introduction

Owing in part to recent development of efficient routes to chiral, nonracemic allenes,<sup>[1]</sup> the transition-metal-catalyzed functionalization of allenes has received considerable recent attention.<sup>[2–5]</sup> Cationic gold(I) complexes have proven particularly effective as catalysts for the functionalization of allenes,<sup>[3]</sup> including the cycloaddition of eneallenes and dieneallenes<sup>[4]</sup> and the hydrofunctionalization of allenes with carbon and heteroatom nucleophiles.<sup>[5]</sup> Much of the interest in this latter family of transformations stems from the potential for chirality transfer from axially chiral, nonracemic allenes.<sup>[6]</sup> However, the stereospecificity of these transformations is often compromised by competitive gold(I)-catalyzed racemization of the allene.<sup>[6–9]</sup> In other cases, gold(I)-catalyzed allene racemization has been exploited to realize the stereoconvergent enantioselective hydrofunctionalization of chiral racemic allenes and propargylic acetates.<sup>[10]</sup>

Although the gold(I)-catalyzed racemization of axially chiral allenes is well documented and is generally assumed to occur through formation of achiral gold  $\eta^1$ -allylic cation intermediates,<sup>[7–11]</sup> there is neither direct experimental evidence to support this contention, nor is there experimental data regarding the energetics of allene racemization. For example, variable-temperature NMR spectroscopy analysis of the gold(I)  $\pi$ -4,5-nonadiene complex  $\{(L)Au[\eta^2-n\text{-Pr}(H)C=C(C(H)n\text{-Pr})]^+\text{SbF}_6^-$  [ $L = P(tBu)_2\text{o-binaphthyl}$  (**1a**)] established a lower limit of  $\Delta G^\ddagger_{298} \geq$

17.4 kcal mol<sup>-1</sup> for allene stereomutation, but the onset of intermolecular allene exchange precluded a more exact determination.<sup>[12]</sup> Rather, our understanding of the mechanism and energetics of gold-catalyzed allene racemization is derived primarily from computational studies.<sup>[8,9,11]</sup> Toward the development of an experimentally grounded understanding of the energetics and mechanism of gold-catalyzed allene racemization, we have studied the kinetics of the racemization of axially chiral 1,3-disubstituted aryl allenes catalyzed by gold(I) phosphine complexes, with a focus on the electronic structure of the rate-limiting transition state. Herein we report the results of this study.

## Results

### Kinetics of catalytic racemization

Toward an experimentally grounded understanding of the mechanism of gold-catalyzed allene racemization, we targeted axially chiral 1,3-disubstituted aryl allenes and gold(I) (aryl)-phosphine complexes with an eye toward evaluating the effects of allene and catalyst electron density while minimizing complications associated with steric perturbation of intermediates and transition states. In an initial experiment, a solution of enantiomerically enriched (*R*)-1-(4-bromophenyl)-1,2-butadiene [*(R)*-**2a**, 97% ee] (73 mM) and a catalytic 1:1 mixture of  $(\text{Ph}_3\text{P})\text{AuCl}$  and AgOTf (1.4 mM; 2 mol %) in ethylbenzene was stirred at 25 °C and monitored periodically by HPLC equipped with chiral stationary phase (Table 1). A plot of  $\ln [\text{ee } (\text{R})\text{-2a}]$  versus time was linear to approximately three half-lives with a pseudo-first-order rate constant of  $k_{\text{obs}} = 4.5(\pm 0.1) \times 10^{-4} \text{ s}^{-1}$  (Figure 1, Table 1, entry 1), which established the first-order dependence of the rate on [*(R)*-**2a**].<sup>[13,14]</sup> Neither AgOTf nor

[a] R. J. Harris, K. Nakafuku, Prof. R. A. Widenhoefer

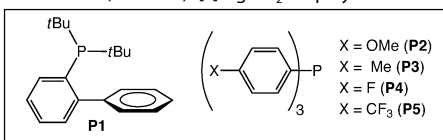
Department of Chemistry, Duke University  
French Family Science Center, Durham, NC, 27708 (USA)  
E-mail: rwideno@chem.duke.edu

 Supporting information for this article is available on the WWW under <http://dx.doi.org/10.1002/chem.201402729>.

**Table 1.** Pseudo-first-order ( $k_{\text{obs}}$ ) and second-order ( $k_{\text{rac}}$ ) rate constants for the gold-catalyzed racemization of aryl allenes (73 mM) at 25 °C.

Entry	R <sup>1</sup>	R <sup>2</sup>	Allene	L	Solvent	Cat. [mM]	$k_{\text{obs}} \times 10^4$ [s <sup>-1</sup> ]	$k_{\text{rac}}$ [M <sup>-1</sup> s <sup>-1</sup> ]
1	Me	Ph	( <i>R</i> )-2 <b>a</b>	PPh <sub>3</sub>	toluene	0.61	14.2 ± 0.2	2.34 ± 0.03
2	Me	Ph	( <i>R</i> )-2 <b>b</b>	PPh <sub>3</sub>	PhEt	0.61	24.8 ± 0.1	4.10 ± 0.02
3	Me	Ph	( <i>R</i> )-2 <b>b</b>	PPh <sub>3</sub>	toluene	0.60	10.2 ± 0.2	1.72 ± 0.03
4	Me	Ph	( <i>R</i> )-2 <b>b</b>	PPh <sub>3</sub>	toluene	0.61	25 ± 2	4.1 ± 0.3
5	Me	Ph	( <i>R</i> )-2 <b>b</b>	PPh <sub>3</sub>	C <sub>6</sub> H <sub>5</sub> Cl	0.65	≥ 547	≥ 85
6	Me	Ph	( <i>R</i> )-2 <b>b</b>	PPh <sub>3</sub>	C <sub>2</sub> H <sub>4</sub> Cl <sub>2</sub>	0.60	≥ 730	≥ 120
7	Me	Br	( <i>R</i> )-2 <b>a</b>	PPh <sub>3</sub>	PhEt	0.72	4.5 ± 0.1	0.62 ± 0.02
8	Me	Br	( <i>R</i> )-2 <b>a</b>	PPh <sub>3</sub>	PhEt	1.4	7.9 ± 0.1	0.55 ± 0.01
9	Me	Br	( <i>R</i> )-2 <b>a</b>	PPh <sub>3</sub>	PhEt	1.4	11.1 ± 0.4	0.78 ± 0.03
10	Me	Br	( <i>R</i> )-2 <b>a</b>	PPh <sub>3</sub>	PhEt	2.9	17.2 ± 0.5	0.59 ± 0.02
11	Me	CO <sub>2</sub> Me	( <i>R</i> )-2 <b>d</b>	PPh <sub>3</sub>	PhEt	10	5.6 ± 0.2	0.056 ± 0.002
12	Me	CN	( <i>R</i> )-2 <b>e</b>	PPh <sub>3</sub>	PhEt	12	2.8 ± 0.1	0.023 ± 0.001
13	Me	NO <sub>2</sub>	( <i>R</i> )-2 <b>c</b>	PPh <sub>3</sub>	PhEt	21	2.3 ± 0.1	0.011 ± 0.001
14	Me	Ph	( <i>R</i> )-2 <b>b</b>	<b>P1</b>	toluene	0.57	4.17 ± 0.03	0.74 ± 0.01
15	Me	CO <sub>2</sub> Me	( <i>R</i> )-2 <b>d</b>	<b>P1</b>	toluene	19	3.6 ± 0.4	0.019 ± 0.002
16	Me	CN	( <i>R</i> )-2 <b>e</b>	<b>P1</b>	toluene	11	0.83 ± 0.02	7.4 ± 0.2 × 10 <sup>-3</sup>
17	Me	NO <sub>2</sub>	( <i>R</i> )-2 <b>c</b>	<b>P1</b>	toluene	19	0.16 ± 0.06	8.3 ± 0.3 × 10 <sup>-4</sup>
18	Me	Ph	( <i>R</i> )-2 <b>b</b>	<b>P2</b>	toluene	0.31	3.57 ± 0.01	1.17 ± 0.01
19	Me	Ph	( <i>R</i> )-2 <b>b</b>	<b>P3</b>	toluene	0.56	17.0 ± 0.9	3.0 ± 0.2
20	Me	Ph	( <i>R</i> )-2 <b>b</b>	<b>P4</b>	toluene	0.94	166 ± 8	17.7 ± 0.9
21	Me	Ph	( <i>R</i> )-2 <b>b</b>	<b>P5</b>	toluene	0.24	410 ± 80	170 ± 30
22	Ph	H	( <i>R</i> )-3 <b>a</b>	PPh <sub>3</sub>	toluene	1.3	16.6 ± 0.4	1.26 ± 0.03
23	Ph	Br	( <i>R</i> )-3 <b>b</b>	PPh <sub>3</sub>	toluene	1.2	3.08 ± 0.05	0.252 ± 0.04
24	Ph	CF <sub>3</sub>	( <i>R</i> )-3 <b>c</b>	PPh <sub>3</sub>	toluene	14	22 ± 2	0.15 ± 0.01
25	Ph	Ph	( <i>R</i> )-3 <b>d</b>	PPh <sub>3</sub>	C <sub>6</sub> H <sub>5</sub> Cl	0.60	55 ± 1	9.30 ± 0.2

[a] Allene enantiopurity is as follows: **2a** = 95% ee, **2b** = 95% ee, **2c** = 91% ee, **2d** = 89% ee, **2e** = 90% ee, **3a** = 98% ee, **3b** = 75% ee, **3c** = 87% ee. [b] Reaction contained tetrabutylammonium triflate (0.40 mM). [c] AgNTf<sub>2</sub> employed as silver source.



(Ph<sub>3</sub>P)AuCl alone catalyzed the racemization of (*R*)-2**a**, consistent with (Ph<sub>3</sub>P)AuOTf as the active catalyst.<sup>[15]</sup>

To determine the rate dependence of allene racemization on catalyst concentration, pseudo-first-order rate constants for the racemization of (*R*)-2**a** catalyzed by (Ph<sub>3</sub>P)AuCl/AgOTf were determined as a function of catalyst concentration from 0.72 to 2.9 mM (Table 1, entries 1–4). A plot of  $k_{\text{obs}}$  versus catalyst concentration was linear (Figure 2) and a plot of  $\log(k_{\text{obs}})$  versus  $\log[\text{catalyst}]$  was linear with a slope of  $1.0 \pm 0.2$  (Figure S1 in the Supporting Information), which together established the first-order dependence of the rate on catalyst concentration and overall the second-order rate law for gold-catalyzed racemization:  $\text{rate} = k_{\text{rac}}[(*R*)-2**a**][(Ph<sub>3</sub>P)AuOTf]$ , where  $k_{\text{rac}} = 0.64(\pm 0.02) \text{ M}^{-1} \text{ s}^{-1}$  ( $\Delta G^\ddagger = 17.7(\pm 0.1) \text{ kcal mol}^{-1}$ ).<sup>[13,14]</sup>

Three sets of experiments were performed to evaluate the effect of allene electron density on the rate of gold-catalyzed racemization. In one set of experiments, pseudo-first-order rate constants were determined for racemization of the *para* substituted 1-aryl-1,2-butadienes (*R*)-2**a**, (*R*)-2**b**, (*R*)-2**c**, (*R*)-2**d**, and (*R*)-2**e** catalyzed by (Ph<sub>3</sub>P)AuCl/AgOTf in ethylbenzene at 25 °C (Table 1, entries 1–8). A plot of  $\log(k_{\text{rac}})$  versus the Hammett  $\sigma^+$  parameter gave a reaction constant of  $\rho^+ = -2.7 \pm 0.2$  (Figure 3). In a second set of experiments, Hammett analysis of the racemization of *para* substituted 1-aryl-1,2-butadienes catalyzed (**P1**)AuCl/AgOTf produced a reaction constant of  $\rho^+ = -2.8 \pm 0.4$  (Table 1, entries 9–12; Figure S2 in the Supporting Information). In a third set of experiments, Hammett analysis of the racemization of the *para* substituted 1-aryl-3-phenylpropadienes (*R*)-Ph(H)C=C(H)(*p*-C<sub>6</sub>H<sub>4</sub>R) [*R*=H (**3a**), Br (**3b**), CF<sub>3</sub> (**3c**)] catalyzed by (Ph<sub>3</sub>P)AuCl/AgOTf produced a reaction constant of  $\rho^+ = -1.49 \pm 0.01$  (Table 1, entries 13–15; Figure 4), which was approximately half the magnitude of that for racemization of 1-aryl-1,2-butadienes catalyzed by (Ph<sub>3</sub>P)AuCl/AgOTf.

To evaluate the effect of phosphine electron-donor ability on the rate of gold-catalyzed allene racemization, pseudo-first-order rate constants were determined for the racemization of (*R*)-2**b** catalyzed by a 1:1 mixture of AgOTf

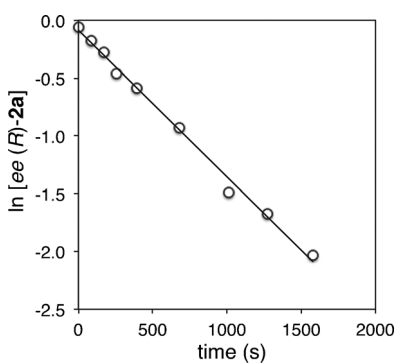


**Figure 1.** Pseudo-first-order plot for the racemization of (*R*)-2**a** (73 mM, 97% ee) catalyzed by a 1:1 mixture of (Ph<sub>3</sub>P)AuCl and AgOTf (1.4 mM) in ethylbenzene at 25 °C.

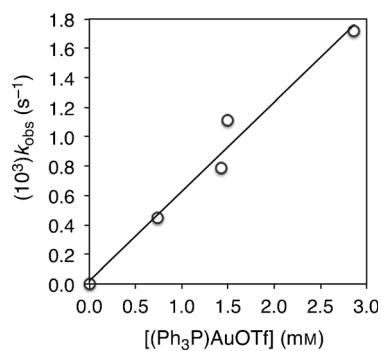


**Figure 2.** Catalyst concentration dependence for the racemization of (*R*)-2**a** (73 mM, 97% ee) catalyzed by a 1:1 mixture of (Ph<sub>3</sub>P)AuCl and AgOTf in ethylbenzene at 25 °C.

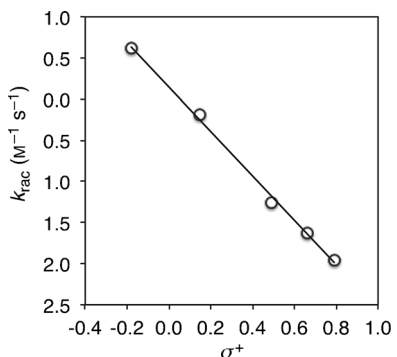


**Figure 3.** Plot of  $\log(k_{\text{rac}})$  versus the Hammett  $\sigma^+$  parameter for the racemization of (R)-2a, (R)-2b, (R)-2c, (R)-2d, and (R)-2e catalyzed by a 1:1 mixture of  $(\text{Ph}_3\text{P})\text{AuCl}$  and  $\text{AgOTf}$  in ethylbenzene at  $25^\circ\text{C}$  ( $\rho^+ = -2.7 \pm 0.2$ ).

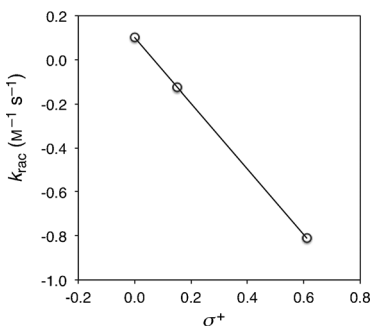


**Figure 4.** Plot of  $\log(k_{\text{rac}})$  versus the Hammett  $\sigma^+$  parameter for the racemization of (R)-3a, (R)-3b, and (R)-3c catalyzed by  $(\text{Ph}_3\text{P})\text{AuCl}/\text{AgOTf}$  ( $\rho^+ = -1.49 \pm 0.01$ ).

and the *para* substituted triarylphosphine gold complexes [ $(4\text{-X-C}_6\text{H}_4)_3\text{P}\text{AuCl}$ ] [X=H, OMe (**P2**), Me (**P3**), F (**P4**), and  $\text{CF}_3$  (**P5**)] (Table 1, entries 5 and 16–19). The second-order rate constant for the racemization of (R)-2b (73 mM) increased by three orders of magnitude as the electron-donor ability of the phosphine decreased from X=OMe (**P2**) to X= $\text{CF}_3$  (**P5**). The corresponding plot of  $\log(k_{\text{rac}})$  versus the Hammett  $\sigma$  parameter provided a reasonable fit ( $R^2=0.9$ ) with a reaction constant of  $\rho=2.5 \pm 0.5$  (Figure 5).

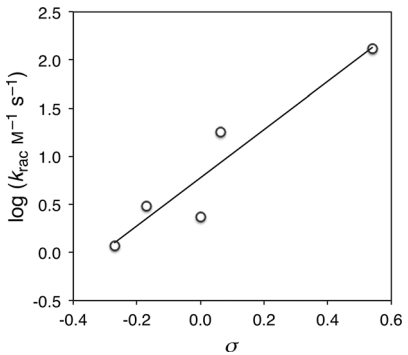


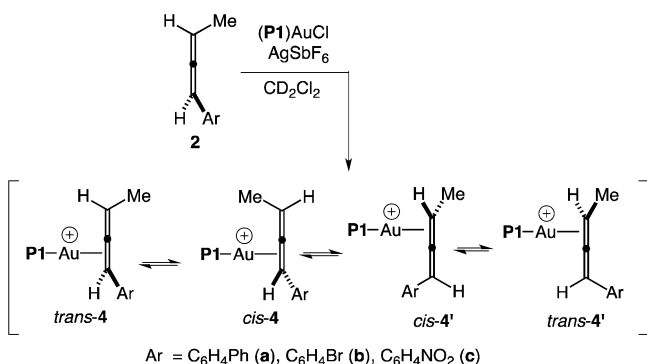
**Figure 5.** Plot of  $\log(k_{\text{rac}})$  versus the Hammett  $\sigma$  parameter for the racemization of (R)-2b catalyzed by  $[(4\text{-C}_6\text{H}_4\text{X})_3\text{P}\text{AuCl}]$  (X=H, Me, OMe, Me, F,  $\text{CF}_3$ ) and  $\text{AgOTf}$  in solvent at  $25^\circ\text{C}$  ( $\rho = 2.5 \pm 0.5$ ).

Several experiments were performed to probe the effect of the counterion and reaction medium on the rate of allene racemization. For example, the second-order rate constants for the racemization of (R)-2b catalyzed by  $(\text{Ph}_3\text{P})\text{AuCl}/\text{AgNTf}_2$  was not significantly different from  $k_{\text{rac}}$  for the racemization of (R)-2b catalyzed by  $(\text{Ph}_3\text{P})\text{AuCl}/\text{AgOTf}$  in (Table 1, entries 20 and 21). Conversely, racemization of (R)-2b catalyzed by  $(\text{Ph}_3\text{P})\text{AuCl}/\text{AgOTf}$  in toluene that contained tetrabutylammonium trifluoromethanesulfonate (40 mM) was approximately two-times faster than in the absence of excess triflate (Table 1, entries 21 and 22). That the rate enhancement caused by excess triflate was due to the concomitant increase in solvent polarity was suggested by the pronounced dependence of the rate of allene racemization on solvent polarity (Table 1, entries 5, 21, 23, and 24). For example, whereas the second-order rate constants for the racemization of (R)-2b catalyzed by  $(\text{Ph}_3\text{P})\text{AuCl}/\text{AgOTf}$  at  $25^\circ\text{C}$  in ethylbenzene ( $\varepsilon=2.41$ ) differed by less than a factor of two from  $k_{\text{rac}}$  for racemization in toluene ( $\varepsilon=2.38$ ), the second-order rate constants for the racemization (R)-2b in chlorobenzene ( $\varepsilon=5.62$ ) or 1,2-dichloroethane ( $\varepsilon=10.36$ ) were  $\geq 36$ - and  $\geq 50$ -times faster, respectively, than was  $k_{\text{rac}}$  for the racemization of (R)-2b in toluene. Similarly, racemization of the 1,3-diarylpropadiene (R)-3a catalyzed by  $(\text{Ph}_3\text{P})\text{AuCl}/\text{AgOTf}$  in chlorobenzene was approximately nine-times faster than was racemization of (R)-3a in toluene (Table 1, entries 13 and 25).

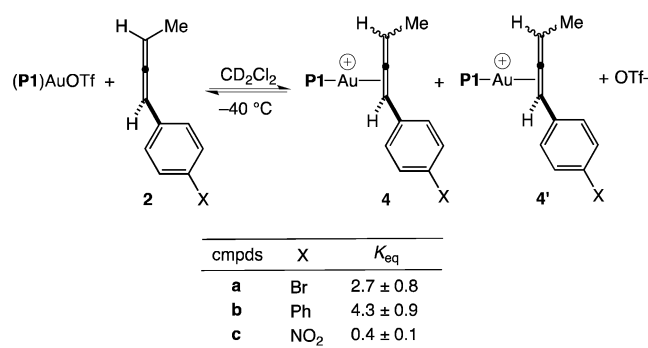
### Gold allene complexes

Although a small number of cationic gold(I)  $\pi$ -allene complexes have been isolated or generated *in situ*,<sup>[12,16]</sup> complexes that contain an aryl allene are not among these. We, therefore, sought to gain an understanding of the electronic structure and behavior of gold 1-aryl-1,2-butadiene complexes germane to the present study. We have previously noted the difficulties associated with the characterization of gold  $\pi$ -complexes containing a triphenylphosphine ligand owing to the poor thermal stability, sluggish ionization, and facile ligand exchange of these complexes.<sup>[16]</sup> We, therefore, targeted complexes containing the *o*-biphenylphosphine ligand **P1** and, to this end, the gold  $\pi$ -allene complexes  $\{(\text{P1})\text{Au}[\eta^2\text{-Me(H)}=\text{C}=\text{C}(\text{H})\text{Ar}]\}^+\text{SbF}_6^-$  [ $\text{Ar}=4\text{-C}_6\text{H}_4\text{Br}$  (**4a**),  $4\text{-C}_6\text{H}_4\text{Ph}$  (**4b**),  $4\text{-C}_6\text{H}_4\text{NO}_2$  (**4c**)] were generated by treatment of the corresponding allene with a 1:1 mixture of  $(\text{P1})\text{AuCl}$  and  $\text{AgSbF}_6$  at  $-80^\circ\text{C}$  in  $\text{CD}_2\text{Cl}_2$  and were characterized by NMR spectroscopy without isolation (Scheme 1).

The  $^{31}\text{P}$  NMR spectra of phosphine complexes **4a–4c** at  $-45^\circ\text{C}$  each displayed a single sharp resonance in the range expected for cationic  $(\text{P1})\text{Au}$   $\pi$ -complexes ( $\delta=64.6$ – $66.7$ ).<sup>[12,17–19]</sup> Cooling these solutions to  $-80^\circ\text{C}$  led to no significant broadening of these resonances, which indicates that complexes **4a–4c** either exist predominantly as a single regio- and diastereomer in solution and/or that intramolecular  $\pi$ -face exchange is rapid on the NMR time scale. We have previously shown that the *cis* and *trans* isomers of the 4,5-nonadiene complex  $\{(\text{P1})\text{Au}[\eta^2\text{-n-Pr(H)}\text{C}=\text{C}(\text{H})\text{n-Pr}]\}^+\text{SbF}_6^-$  (**1b**) differ in energy by  $<0.5 \text{ kcal mol}^{-1}$  and interconvert rapidly ( $\Delta G^\ddagger =$



Ar = C<sub>6</sub>H<sub>4</sub>Ph (**a**), C<sub>6</sub>H<sub>4</sub>Br (**b**), C<sub>6</sub>H<sub>4</sub>NO<sub>2</sub> (**c**)



**Scheme 2.** Equilibrium binding affinities of allenes **2a–2c** to the (P1)Au<sup>+</sup> fragment relative to triflate anion.

9.7 kcal mol<sup>-1</sup>) via intramolecular  $\pi$ -face exchange,<sup>[12]</sup> which suggests that complexes **4** exist as rapidly interconverting mixtures of *cis* and *trans* diastereomers and C1=C2- and C2=C3-bound regioisomers (Scheme 1). In the <sup>1</sup>H NMR spectra of **4b**, the C1 allenyl proton resonance was shifted upfield [ $\Delta\delta(\text{H}1) = -0.34$ ] while the C3 allene proton resonance was shifted downfield [ $\Delta\delta(\text{H}3) = 0.21$ ] relative to free allene. Comparison of these data to the spectra of known [(P1)Au( $\pi$ -allene)]<sup>+</sup> complexes<sup>[12]</sup> suggests that the allene ligand of **4b** binds to gold preferentially through the C1=C2 bond (Scheme 1). Similar, albeit attenuated, perturbation of allene chemical shifts were observed for complex **4a** [ $\Delta\delta(\text{H}1) = -0.24$ ,  $\Delta\delta(\text{H}3) = 0.10$ ]. Conversely, for complex **4c** containing the more electron-deficient *p*-nitrophenyl-substituted allene, the C1 allenyl proton resonance was shifted slightly downfield [ $\Delta\delta(\text{H}1) = 0.08$ ] while the C3 allene proton resonance was shifted upfield [ $\Delta\delta(\text{H}3) = -1.01$ ] relative to free allene suggesting preferential binding of the allene to gold via the C2=C3 bond (Scheme 1).

The electronic dependence of vinyl arene binding affinities has been utilized to evaluate the relative contributions of  $\sigma$ -donation and  $\pi$ -backbonding to the metal–alkene bond, and hence the electrophilicity of unsaturated metal fragments.<sup>[17,20–23]</sup> We sought to evaluate the electronic structure of the Au–( $\pi$ -allene) interaction in complexes **4** employing an analogous approach. To this end, we determined equilibrium constants for the displacement of triflate from (P1)AuOTf with allenes (*R*)-**2a**, (*R*)-**2b**, and (*R*)-**2c** at -40 °C (Scheme 2). A plot of log( $K_{\text{eq}}$ ) versus the Hammett  $\sigma$  parameter produced a reaction constant of  $\rho = -1.4 \pm 0.1$  (Figure 6), which reveals the depletion of electron density from the allene upon complexation to gold. However, because the population of the C1=C2 regioisomer decreases with the decreasing electron-donor ability of the 1-aryl group and because the binding affinity of the C2=C3 regioisomer is presumably not significantly affected by the electronic nature of the C1 aryl group, the reaction constant of  $\rho = -1.4 \pm 0.1$  represents the lower limit (numerically most positive) of the extent of electron depletion from the C1 allene carbon upon complexation to the (P1)Au<sup>+</sup> fragment. Supporting this contention, we previously determined a reaction constant of  $\rho = -3.4 \pm 0.2$  for the equilibrium binding affinities of substituted vinyl arenes to the (P1)Au<sup>+</sup>.<sup>[17]</sup>

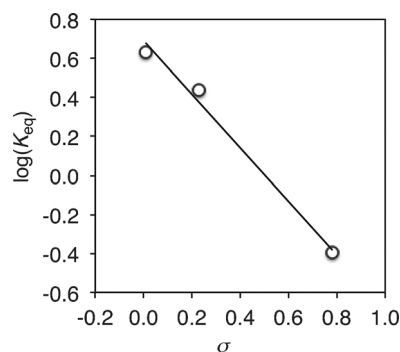


**Figure 6.** Plot of  $K_{\text{eq}}$  versus the Hammett  $\sigma$  parameter for the equilibrium displacement of OTf<sup>-</sup> from (P1)AuOTf with 1-aryl-1,2-butadienes **2a**, **2b**, and **2c** in CD<sub>2</sub>Cl<sub>2</sub> at -40 °C ( $\rho = -1.4 \pm 0.1$ ).

To determine the energetics of intermolecular allene exchange with gold ( $\pi$ -1-aryl-1,2-butadiene) complexes **4**, we determined pseudo-first-order rate constants for the intermolecular exchange of allene **2a** with complex **4a** (33 mM) as a function of [2a] from 4.0 to 24 mM at -40 °C employing <sup>1</sup>H NMR spin-saturation transfer techniques.<sup>[24]</sup> A plot of  $k_{\text{obs}}$  versus [2a] was linear with a significant nonzero intercept, which established the two-term rate law for intermolecular allene exchange: rate =  $k_1[\mathbf{4a}] + k_2[\mathbf{4a}][\mathbf{2a}]$ , where  $k_1 = 0.94 \pm 0.01$  s<sup>-1</sup> ( $\Delta G^\ddagger = 13.5$  kcal mol<sup>-1</sup>) and  $k_2 = 13.0 \pm 0.5$  M<sup>-1</sup> s<sup>-1</sup> ( $\Delta G^\ddagger = 12.3$  kcal mol<sup>-1</sup>; Figure S3 in the Supporting Information).

## Discussion

### Catalyzed and uncatalyzed allene racemization

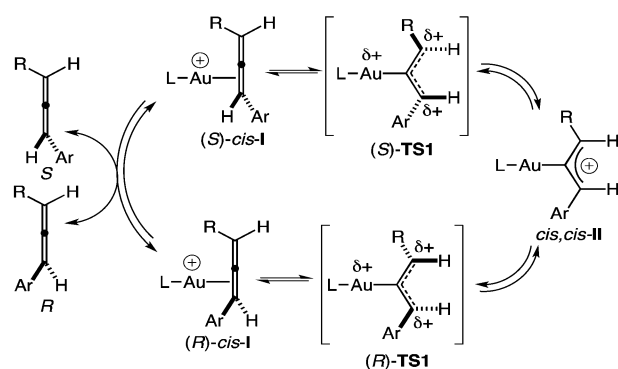
1,3-Dialkyl allenes racemize thermally in the absence of catalysts via an allyl diradical intermediate with energy barriers of approximately 46 kcal mol<sup>-1</sup>,<sup>[25]</sup> and this process is often accelerated by photosensitizers.<sup>[26]</sup> In addition to gold(I) complexes,<sup>[7–11]</sup> a small number of transition-metal complexes racemize allenes. Claessen reported the racemization of simple allenes by organocuprates and suggested a mechanism involving radical anion intermediates.<sup>[27]</sup> Bäckvall and Horváth reported the Pd<sup>II</sup>-catalyzed racemization of allenes in the presence of

LiBr, which was proposed to occur by reversible addition of bromide to the central carbon atom of the allene to generate an equilibrating mixture of  $\sigma$ - and  $\pi$ -allyl palladium complexes.<sup>[28]</sup> Morken<sup>[29]</sup> and Molander<sup>[30]</sup> have documented the Pd<sup>0</sup>-catalyzed racemization of allenes although no mechanisms were proposed. Cramer<sup>[31]</sup> and Willis<sup>[32]</sup> have reported the rhodium-catalyzed racemization of allenes, which Cramer proposed to occur via allene hydro-metallation, isomerization through a rhodium-allyl species, and subsequent elimination. In addition to these catalytic processes, planar  $\eta^1$ -allylic cation intermediates have been invoked to account for the stereomutation of chiral iron,<sup>[33]</sup> platinum,<sup>[34]</sup> and silver<sup>[35]</sup> allene complexes. Bergman reported the stoichiometric stereoinversion and racemization of 1,3-disubstituted allenes by a zirconocene imido complex that was proposed to occur through stereospecific [2+2] cycloaddition followed by racemization of the resulting azazirconacyclobutane.<sup>[36]</sup>

### Mechanism of gold-catalyzed allene racemization

All our experimental observations and available information regarding the racemization of axially chiral aryl allenes catalyzed by gold phosphine complexes are consistent with a mechanism involving rapid and reversible interconversion of the enantio-, diastereo-, and regioisomeric gold  $\eta^2$ -allene complexes I followed by turnover-limiting, unimolecular conversion of cis-I to the achiral  $\eta^1$ -allylic cation intermediate cis,cis-II via the bent and twisted  $\eta^1$ -allene transition state cis,cis-TS1 (Scheme 3). Although our experimental data do not distinguish between the potential diastereomers of  $\eta^1$ -allylic cation II and transition state TS1, computational analysis of gold(I)  $\eta^1$ -1,3-disubstituted allylic cations<sup>[8,9,11]</sup> and experimental<sup>[37,38]</sup> and computational<sup>[39]</sup> analysis of 1,3-disubstituted allylic cations all point to preferential formation of  $\eta^1$ -allylic cation cis,cis-II owing to the unfavorable steric interactions associated with *endo* substituents on an allylic cation. Similar steric interactions in the transition state presumably disfavor trans,trans-TS1 and cis,trans-TS1 relative to cis,cis-TS1, which in turn implicates cis-I as the reactive  $\eta^2$  allene complex (Scheme 3). Owing to the significant conjugative stabilization of a planar allylic cation relative to the perpendicular conformation,<sup>[39]</sup> estimated to be approximately 15 kcal mol<sup>-1</sup> in the case of the 1-phenyl-3-methyl allylic cation,<sup>[38]</sup> allylic cation cis,cis-II likely represents a local minimum on the reaction coordinate.

The energy barriers for intermolecular  $\pi$ -ligand exchange of cationic (triphenylphosphine)gold  $\pi$ -alkyne complexes ( $\Delta G^\ddagger \approx 9$  kcal mol<sup>-1</sup>)<sup>[16]</sup> and  $\pi$ -allene complex 4a ( $\Delta G^\ddagger = 12.3$  kcal mol<sup>-1</sup>) are significantly lower than are the energy barriers for catalytic allene racemization ( $\Delta G^\ddagger = 17.0$ –21.6 kcal mol<sup>-1</sup>). Similarly, we have shown that the cis and trans isomers of the 4,5-nonadiene complex  $\Delta G^\ddagger$  differ in energy by <0.5 kcal mol<sup>-1</sup> and interconvert rapidly ( $\Delta G^\ddagger < 10$  kcal mol<sup>-1</sup>) via intramolecular  $\pi$ -face exchange.<sup>[12]</sup> The variable-temperature NMR behavior of allene complexes 4 was likewise in accord with rapid interconversion of the potential  $\pi$ -allene regio- and diastereomers via intramolecular  $\pi$ -face exchange. For these reasons, we can confidently rule out mechanisms for allene racemiza-



**Scheme 3.** Proposed mechanism for the gold-catalyzed racemization of aromatic allenes.

tion involving turnover-limiting intermolecular or intramolecular allene exchange. Although  $K_{eq}$  for the displacement of triflate anion from (P1)AuOTf by 1-aryl-1,2-butadienes at  $-40^\circ\text{C}$  was nearly thermoneutral, the large allene/triflate ratio employed under catalytic conditions and the absence of any inhibitory effect of triflate anion on the rate of racemization ensures that gold  $\eta^2$ -allene complexes I represent the predominant species present under catalytic conditions.

Although the rate of gold-catalyzed racemization of (R)-2b increased in the presence of excess triflate, we can safely rule out a mechanism for allene racemization involving rate-limiting attack of triflate ion at the C2 allene carbon atom of a gold  $\eta^2$ -allene complex, as has been invoked for Pd<sup>0</sup>-catalyzed allene racemization.<sup>[28]</sup> In particular, the negative reaction constants for the racemization of 1-aryl-1,2-butadienes ( $\rho^+ = -2.7$ –2.8) and 1-phenyl-3-aryl-1,2-propadienes ( $\rho^+ = -1.5$ ) established the depletion of electron density from the terminal allene carbon atoms in the transition state for racemization relative to the ground state  $\eta^2$ -allene complex. A mechanism involving nucleophilic attack at the C2 allene carbon of an  $\eta^2$ -allene complex would lead to the accumulation of electron density on allene in the transition state for racemization relative to the ground state, which is opposite the effect observed experimentally. Rather, the observed dependence of the rate of allene racemization on triflate concentration can be attributed to the concomitant increase in solvent polarity, which had a pronounced affect on reaction rate (see below).

### Electronic structure of the rate-limiting transition state

All of our experimental observations are in accord with a transition state for allene racemization (cis,cis-TS1) that resembles a bent and twisted  $\eta^1$ -allene complex with diminished electron density on the terminal allene carbon atoms and increased electron density on the phosphine ligand relative to the ground state  $\eta^2$ -allene complex. In addition to the negative reaction constants for gold-catalyzed racemization of 1-aryl-1,2-butadienes ( $\rho^+ = -2.7$ –2.8) and 1-phenyl-3-aryl-1,2-propadienes ( $\rho^+ = -1.5$ ), the large positive reaction constant ( $\rho = 2.5$ ) for the racemization of (R)-2b catalyzed by *p*-substituted triarylphosphine complexes (L)AuOTf (L = PPh<sub>3</sub>, P2–P5) estab-

lished the accumulation of electron density on the phosphorous atom in the transition state for racemization relative to the ground state  $\eta^2$ -allene complex. Together, these data establish the net transfer of electron density from the allene to the (L)Au moiety in the conversion of ground state to the transition state for racemization.

The diminished reaction constant for racemization of 1-phenyl-3-arylpropadienes ( $\rho^+ = -1.5$ ) relative to 1-aryl-1,2-butadienes ( $\rho^+ = -2.7$ – $-2.8$ ) established the lower electron demand of the aryl-bound allene carbon atom in the transition state for racemization of 1-phenyl-3-arylpropadienes relative to 1-aryl-1,2-butadienes. This observation suggests that distribution of positive charge between the terminal allene carbon atoms in transition state **TS1** is varied and depends on the relative electron-releasing abilities of the allene C1 and C3 substituents. It is worth noting that the second-order rate constants ( $k_{\text{rac}}$ ) for racemization of *(R)*-**3b** and *(R)*-**2a**, both of which contain a terminal *p*-bromophenyl substituent, differed by only approximately 20% despite the superior electron-donor properties of the phenyl group of *(R)*-**3b** relative to the methyl group of *(R)*-**2a**. This observation points to steric destabilization of transition state **TS1** by the terminal phenyl group of *(R)*-**3b** relative to the terminal methyl substituent of *(R)*-**2a**.

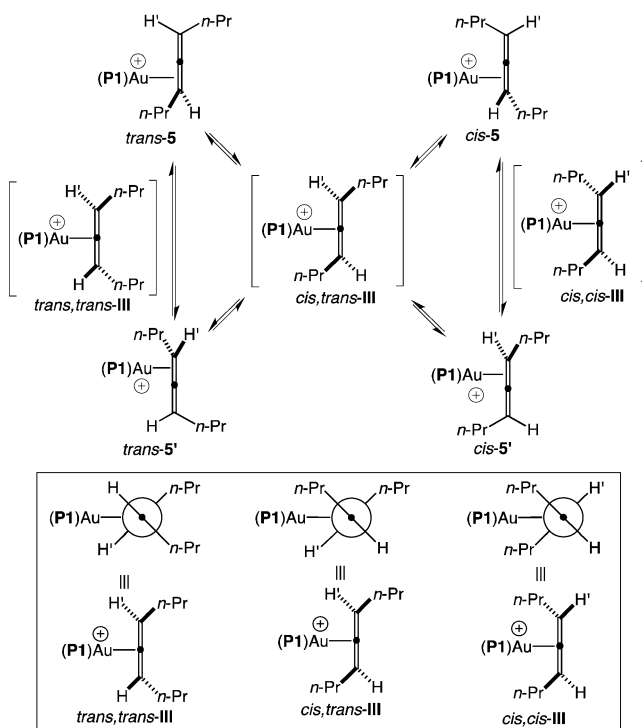
The reaction constants determined for the gold-catalyzed racemization of 1-aryl-1,2-butadienes and 1,3-diaryl-1,2-propadienes are less negative than those determined for the hydrochlorination of 1-aryl-1,2-propadienes ( $\rho^+ = -4.20$ )<sup>[40]</sup> and 1-aryl-1,3-butadienes ( $\rho^+ = -2.98$ )<sup>[38]</sup> in glacial acetic acid and for the solvolysis of 1,3-diaryl-3-chloro-1-propenes ( $\rho^+ = -3.1$ )<sup>[41]</sup> in 60% aqueous acetone, particularly considering the nonpolar reaction medium employed for gold-catalyzed allene racemization. These comparisons suggest that significant positive charge resides on the allene ligand of the ground state  $\eta^2$ -allene complex for allene racemization. Indeed, the negative reaction constant ( $\rho = -1.4$ ) determined for the equilibrium binding affinities of 1-aryl-1,2-butadienes to the **(P1)Au<sup>+</sup>** fragment established depletion of electron density from the C1 atom of bound allene relative to free allene. Furthermore, our previous determination of a reaction constant of  $\rho = -3.4$  for binding of *p*-substituted vinyl arenes to the **(P1)Au<sup>+</sup>** fragment suggests the reaction constant  $\rho = -1.4$  significantly underestimates the extent of electron depletion from the allene upon binding to gold.<sup>[17]</sup>

The observations noted in the preceding paragraph point to the central role of  $\pi$ -activation in gold-catalyzed allene racemization, a contention that is further supported by the large positive reaction constant ( $\rho = 2.5$ ) for the racemization of *(R)*-**2b** catalyzed by *p*-substituted triarylphosphine gold complexes. In this regard, it is worth noting that we have previously documented the markedly greater electrophilicity of the twelve-electron **(P1)Au<sup>+</sup>** fragment relative to cationic Ag<sup>+</sup>, Pd<sup>II</sup>,<sup>[21]</sup> and Pt<sup>II</sup><sup>[22]</sup> complexes through analysis of vinyl arene relative binding affinities.<sup>[17]</sup> Therefore, to the extent that allene racemization reactivity tracks with the electrophilicity of the metal complex, these data provide a rationale for the high reactivity of cationic gold(I) complexes relative to related late transition metal complexes as allene racemization catalysts.

Analysis of solvent effects provides further insight into the distribution of charge in the transition state for allene racemization. Because racemization occurs without the creation or consumption of charge, the strong dependence of the rate of racemization of 1-aryl-1,2-butadienes on solvent polarity (in particular the  $\geq 50$ -fold increase in reaction rate for racemization of *(R)*-**2b** in 1,2-dichloroethane relative to toluene) points to the localization of positive charge in the transition state relative to the ground state.<sup>[42]</sup> More specifically, these observations suggest that in the ground state  $\eta^2$ -allene complex, positive charge is dispersed across the gold atom and phosphine and allene ligands and becomes localized on the C1 allene terminus in the transition state for racemization. In support of the former contention, computational analysis of gold  $\pi$ -complexes  $\{(\text{Ph}_3\text{P})\text{Au}[\eta^2-\text{H}_2\text{C}=\text{C}(\text{H})-4-\text{C}_6\text{H}_4\text{Me}]\}^+$  and  $\{(\text{Ph}_3\text{P})\text{Au}(\eta^2-\text{MeC}\equiv\text{CMe})\}^+$  indicates more than 60% of the positive charge resides on the phosphine and  $\pi$ -ligands.<sup>[43]</sup> The significantly attenuated effect of solvent polarity on the rate of racemization of 1-phenyl-1,2-propadienes relative to 1-aryl-1,2-butadienes points to greater delocalization of positive charge in the transition state for racemization of 1-phenyl-1,2-propadienes relative to 1-aryl-1,2-butadienes. This conclusion is in accord with the attenuated reaction constant for the  $(\text{Ph}_3\text{P})\text{AuOTf}$ -catalyzed racemization of 1-phenyl-1,2-propadienes ( $\rho^+ = -1.5$ ) relative to 1-aryl-1,2-butadienes ( $\rho^+ = -2.7$ ), which established more equal distribution of positive charge between the C1 and C3 allene carbon atoms in the transition state for racemization of 1-phenyl-1,2-propadienes relative to 1-aryl-1,2-butadienes.

### Relationship between the $\eta^1$ -allene species involved in stereomutation and $\pi$ -face exchange

Variable temperature NMR analysis of aliphatic gold  $\pi$ -complexes established facile intramolecular  $\pi$ -face exchange of the allene ligand without stereomutation.<sup>[12]</sup> To account for this behavior, we invoked the involvement of chiral,  $\eta^1$ -allene intermediates or transition states **III** in which gold is bound 45° relative to the allene axes, presumably interacting with both *p*-orbitals of the central carbon atom (Scheme 4). Similar chiral  $\eta^1$ -allene species have been invoked to account for  $\pi$ -face exchange in platinum<sup>[44]</sup> and iron<sup>[33,45]</sup>  $\pi$ -allene complexes and gold  $\eta^1$ -allene species have been evaluated computationally.<sup>[8,9]</sup> Germane to the present study, analysis of the 4,5-nonadiene complexes **1a** and **1b** revealed two discrete  $\pi$ -face exchange pathways associated with two diastereomeric  $\eta^1$ -allene intermediates/transition states that lay well below the transition state for allene stereomutation ( $\Delta G^\ddagger = \geq 17.4 \text{ kcal mol}^{-1}$ ).<sup>[12]</sup> a lower energy process ( $\Delta G^\ddagger = 8.8 \text{ kcal mol}^{-1}$ ) involving either the *trans,trans*-**III** or *cis,cis*-**III** that interconverts the allenyl protons of the more stable  $\eta^2$ -allene stereoisomer (*cis*-**5** or *trans*-**5**) and a higher energy process ( $\Delta G^\ddagger = 9.7 \text{ kcal mol}^{-1}$ ) involving *cis,trans*-**III** that interconverts the  $\eta^2$ -allene diastereomers *cis*-**5** and *trans*-**5** (Scheme 4).<sup>[12]</sup> Because these two processes together led to complete interconversion of all four allene protons of both *cis*-**5** and *trans*-**5**, we have no information regarding the energetics of the third  $\eta^1$ -allene diastereomer (*trans,trans*-**III** or *cis,cis*-**III**).



Scheme 4. Pathways for  $\pi$ -face exchange for gold allene complex 5.

From the observations outlined in the preceding paragraph, two scenarios emerge for the relationship between the chiral  $\eta^1$ -allene species III involved in  $\pi$ -face exchange without stereomutation and transition state TS1 leading to allene stereomutation (Figure 7). The first scenario is that both species exist along the reaction coordinate for allene stereomutation with facile  $\pi$ -face exchange occurring via intermediate *cis,cis*-TS1 which is superimposed on slower stereomutation via transition state *cis,cis*-TS1 (Figure 7).<sup>[46]</sup> The second scenario is that a single *cis,cis*- $\eta^1$ -allene species is present along the reaction coordinate for allene stereomutation and there is no  $\pi$ -face exchange without stereomutation, that is, *cis,cis*-III and *cis,cis*-TS1 are the same species (Figure 7). Implicit in this scenario is that the stereochemical fidelity of the  $\eta^1$ -allene species III is dependent on stereochemical configuration and whereas  $\eta^1$ -allene species *trans,trans*-III and *cis,trans*-III maintain configurational stability throughout  $\pi$ -face exchange, *cis,cis*- $\eta^1$ -III does not. Implicit in both these scenarios is that *cis,cis*-III is the highest energy  $\eta^1$ -allene species involved  $\pi$ -face exchange, although as noted above, our data do not distinguish between *cis,cis*-III and *trans,trans*-III.

Of the two mechanistic scenarios outlined in the preceding paragraph and depicted in Figure 7, we favor the former involving two discrete  $\eta^1$ -allene species along the reaction coordinate for allene stereomutation. This contention is based on the nominal effect that allene configuration has on the stabilities of the chiral  $\eta^1$ - and  $\eta^2$ -allene complexes involved in the  $\pi$ -face exchange of 1b. Specifically, the two lowest energy chiral  $\eta^1$ -allene complexes, *cis,trans*-III and presumably *trans,trans*-III, differ in energy by  $< 1 \text{ kcal mol}^{-1}$  and the  $\eta^2$ -allene diastereomers *cis*-5 and *trans*-5 differ in energy by  $< 0.5 \text{ kcal mol}^{-1}$ .

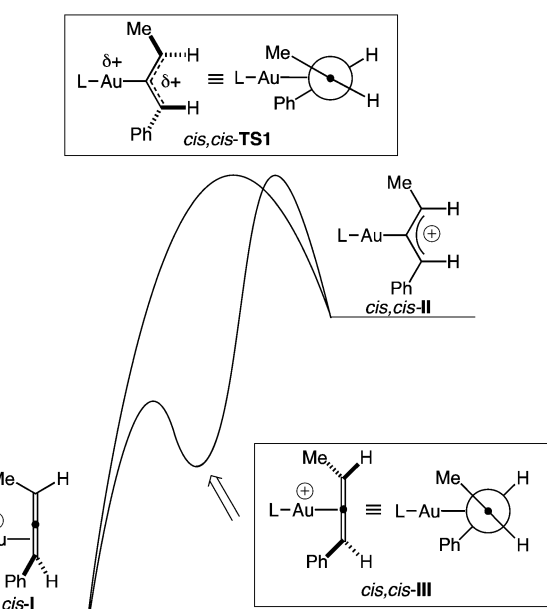


Figure 7. Reaction coordinate diagram for allene stereomutation via transition state *cis,cis*-TS1 with and without the intermediacy of the chiral  $\eta^1$ -allene species *cis,cis*-III.

These observations indicate that the *cis* or *trans* orientation of the allene substituents have no significant effect on the stability of the  $\eta^1$ - and  $\eta^2$ -allene species. It therefore appears unlikely that the highest energy  $\eta^1$ -allene diastereomer, presumably *cis,cis*-III, would be destabilized by  $\geq 7.5 \text{ kcal mol}^{-1}$  relative to *cis,trans*-III.

#### Comparison of experiment and computation

Notable among the computational analyses of gold-catalyzed allene racemization are the DFT analyses of the stereomutation of gold(I) 2,3-pentadiene complexes  $\{(L)\text{Au}[\pi\text{-Me(H)}\text{C}=\text{C(H)Me}]\}^+$  [ $L = \text{PPh}_3$ ,<sup>[8]</sup>  $\text{PMe}_3$ <sup>[9]</sup>] and related complexes.<sup>[12]</sup> These studies invoke mechanisms involving unimolecular isomerization of the chiral  $\eta^2$ -allene complex A to the planar  $\eta^1$ -allylic cation complex B via the bent and twisted  $\eta^1$ -allene transition state C with energy barriers of  $< 12 \text{ kcal mol}^{-1}$  (Figure 8). These calculations predict that relative to ground state A,<sup>[46]</sup> transition state C displays more pronounced bending ( $\text{C}_1\text{-C}_2\text{-C}_3 = 130\text{--}140^\circ$ ) and twisting ( $\text{Me-C}_1\text{-C}_3\text{-Me} = 50\text{--}65^\circ$ ) of the  $\text{C}=\text{C}=\text{C}$  moiety with accumulation of positive charge on both terminal allenyl carbon atoms and diminished charge on the gold atom (Figure 8). Computational analysis of the 1,2,4-pentatriene complex  $\{(\text{Me}_3\text{P})\text{Au}[\pi\text{-Me(H)}\text{C}=\text{C(H)CH=CH}_2]\}^+$  (6) predicts that the conjugated vinyl group stabilizes both the bent  $\eta^1$ -allene species C and  $\eta^1$ -allylic cation B relative to  $\eta^2$ -allene complex A to the extent that allylic cation B becomes the ground state, lying  $1.0 \text{ kcal mol}^{-1}$  below A and  $2.3 \text{ kcal mol}^{-1}$  below C.<sup>[9]</sup>

The computationally predicted transition state for stereomutation of gold(I) 2,3-pentadiene complexes appears consistent with our experimental observations, in particular the depletion

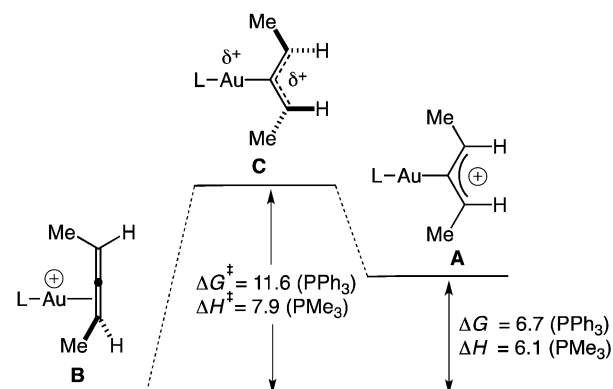


**Figure 8.** Computationally predicted reaction coordinate for the stereomutation of gold allene complexes  $\{(\text{L})\text{Au}[\pi\text{-Me}(\text{H})\text{C}=\text{C}(\text{H})\text{Me}]\}^+$  ( $\text{L}=\text{PPh}_3^{[8]}, \text{PMe}_3^{[9]}$ ). Energy values in  $\text{kcal mol}^{-1}$ .

of electron density on the terminal allene carbon atoms and the accumulation of electron density of the  $(\text{L})\text{Au}$  fragment relative to the ground state  $\eta^2$ -allene complex. However, as we have noted previously,<sup>[13]</sup> there appears to be a significant discrepancy regarding the computationally predicted ( $8\text{--}12 \text{ kcal mol}^{-1}$ ) and experimentally determined ( $\Delta G^\ddagger \geq 17.4 \text{ kcal mol}^{-1}$ ) energy barriers for stereomutation of a 1,3-dialkylallene. Similarly, comparison of the experimentally determined energy barrier for the racemization of **(R)-2b** in toluene ( $\Delta G^\ddagger = 16.9 \text{ kcal mol}^{-1}$ ) relative to the structures calculated for the 1,2,4-pentatriene complex **6** suggests that computation also over estimates the extent to which a conjugated group stabilizes the bent  $\eta^1$ -allene species and  $\eta^1$ -allylic cation, with the caveat that the phenyl group of **(R)-2a** might sterically destabilize the transition state for allene stereomutation relative to the vinyl group of **6**. Also worth noting is that computation gives no indication of the existence of two types of  $\eta^1$ -allene complexes. Computation does indeed predict that the bent *cis,trans*- and *trans,trans*- $\eta^1$ -allene transition states collapse to the corresponding  $\eta^2$ -allene complexes without stereomutation, but also predicts that these transition states are higher in energy than is the bent *cis,cis*- $\eta^1$ -allene transition state leading to stereomutation.<sup>[8, 9, 12]</sup>

## Conclusions

We have analyzed the kinetics of the racemization of 1-aryl-1,2-butadienes and 1-aryl-3-phenyl-propadienes catalyzed by cationic gold(I) phosphine complexes. The results of this study are consistent with a mechanism for racemization involving rapid and reversible inter- and intramolecular allene exchange followed by turnover-limiting, unimolecular conversion of a chiral *cis*- $\eta^2$ -allene complex (*cis*-I) to an achiral *cis,cis*- $\eta^1$ -allylic cation intermediate (*cis,cis*-II) via a bent and twisted  $\eta^1$ -allene transition state (*cis,cis*-TS1). In a nonpolar solvent, such as toluene, energy barriers for allene racemization range from  $\Delta G^\ddagger = 16.9 \text{ kcal mol}^{-1}$  for racemization of 1-(4-biphenyl)-1,2-butadiene [**(R)-2b**] catalyzed by  $(\text{Ph}_3\text{P})\text{AuCl}/\text{AgOTf}$  to  $\Delta G^\ddagger = 21.6 \text{ kcal mol}^{-1}$  for racemization of 1-(4-nitrophenyl)-1,2-butadiene [**(R)-2c**] catalyzed by  $(\text{P1})\text{AuCl}/\text{AgOTf}$ . The free energy of the former transformation is lowered by  $\Delta\Delta G^\ddagger \geq 2 \text{ kcal mol}^{-1}$  in the more polar solvent 1,2-dichloroethane.

Hammett analysis of the gold-catalyzed racemization of aryl allenes as a function of both the allene and phosphine ligand established the depletion of electron density on the terminal allene carbon atoms and the accumulation of electron density on the phosphorous atom in the transition state for stereomutation relative to ground state  $\eta^2$ -allene complex. Comparison of the effects of solvent polarity and allene electron density on the rate of racemization of 1-aryl-1,2-butadienes and 1-aryl-3-phenyl-propadienes indicates that in the former case, positive charge is localized on the C1 allene position in the transition state for stereomutation while in the latter case, positive charge is more evenly distributed between the C1 and C3 allene positions in the transition state for stereomutation. These data also point to the significant delocalization of positive charge onto the phosphine and allene ligands in the ground state  $\eta^2$ -allene complex. The depletion of electron density from the allene in the ground state  $\eta^2$ -allene complex appears largely responsible for the high reactivity of cationic gold(I) complexes as catalysts for allene racemization.

Our experimental observations regarding the effect of the supporting ligand donor ability and solvent polarity on the rates of gold(I)-catalyzed allene racemization provide additional criteria to be considered in the proper selection of supporting ligand and reaction medium for the gold(I)-catalyzed functionalization of axially chiral allenes. However, as is the case with allene racemization, the rate of nucleophilic addition to a gold(I)  $\pi$ -allene complex likely increases with the decreasing electron-donor ability of the supporting ligand and increasing polarity of the solvent.<sup>[47]</sup> For this reason, it appears unlikely that a simple relationship exists between the electron-donor ability of the ligand and solvent polarity and the extent of chirality transfer, or conversely, the extent of allene racemization in the gold(I)-catalyzed functionalization of axially chiral allenes.

## Acknowledgements

We acknowledge the NSF (CHE-1213957) for support of this research. Support for R.J.H. was provided through a Kathleen Zeilek fellowship provided by Duke University.

**Keywords:** allenes • allylic compounds • gold • pi complexes • racemization

- [1] a) S. Ma, *Eur. J. Org. Chem.* **2004**, 1175–1183; b) A. Barbero, F. J. Pulido, *Synthesis* **2004**, 779–785; c) N. Krause, A. Hoffmann-Röder, *Tetrahedron* **2004**, 60, 11671–11694; d) K. M. Brummond, J. E. DeForrest, *Synthesis* **2007**, 795–818; e) M. Ogasawara, *Tetrahedron: Asymmetry* **2009**, 20, 259–271; f) S. Yu, S. Ma, *Chem. Commun.* **2011**, 47, 5384–5418; g) T. Hashimoto, K. Sakata, F. Tamakuni, M. J. Dutton, K. Maruoka, *Nat. Chem.* **2013**, 5, 240–244.
- [2] a) S. Yu, S. Ma, *Angew. Chem.* **2012**, 124, 3128–3167; *Angew. Chem. Int. Ed.* **2012**, 51, 3074–3112; b) A. Deagostino, C. Prandi, S. Tabasso, P. Venturello, *Molecules* **2010**, 15, 2667–2685; c) F. López, J. L. Mascareñas, *Chem. Eur. J.* **2011**, 17, 418–428; d) C. Aubert, L. Fensterbank, P. Garcia, M. Malacia, A. Simonneau, *Chem. Rev.* **2011**, 111, 1954–1993; e) F. Ina-

- gaki, S. Kitagaki, C. Mukai, *Synlett* **2011**, 594–614; f) B. Alcaide, P. Almendros, T. Martínez del Campo, E. Soriano, J. Marco-Contelles, *Top. Curr. Chem.* **2011**, 302, 183–224.
- [3] a) N. Krause, C. Winter, *Chem. Rev.* **2011**, 111, 1994–2009; b) M. Bandini, *Chem. Soc. Rev.* **2011**, 40, 1358–1367.
- [4] a) H. C. Shen, *Tetrahedron* **2008**, 64, 7847–7870; b) F. López, J. L. Mascareñas, *Beilstein J. Org. Chem.* **2011**, 7, 1075–1094; c) F. López, J. L. Mascareñas, *Beilstein J. Org. Chem.* **2013**, 9, 2250–2264; d) D. Garayalde, C. Nevado, *ACS Catal.* **2012**, 2, 1462–1479.
- [5] A. S. K. Hashmi, M. Buehrle, *Aldrichimica Acta* **2010**, 43, 27–33.
- [6] a) N. T. Patil, *Chem. Asian J.* **2012**, 7, 2186–2194; b) N. Bongers, N. Krause, *Angew. Chem.* **2008**, 120, 2208–2211; *Angew. Chem. Int. Ed.* **2008**, 47, 2178–2181.
- [7] a) N. Nishina, Y. Yamamoto, *Angew. Chem.* **2006**, 118, 3392–3395; *Angew. Chem. Int. Ed.* **2006**, 45, 3314–3317; b) N. T. Patil, L. M. Lutete, N. Nishina, Y. Yamamoto, *Tetrahedron Lett.* **2006**, 47, 4749–4751; c) Z. Zhang, C. Liu, R. E. Kinder, X. Han, H. Qian, R. A. Widenhoefer, *J. Am. Chem. Soc.* **2006**, 128, 9066–9073; d) Z. Liu, A. S. Wasmuth, S. G. Nelson, *J. Am. Chem. Soc.* **2006**, 128, 10352–10353; e) N. Morita, N. Krause, *Angew. Chem.* **2006**, 118, 1930–1933; *Angew. Chem. Int. Ed.* **2006**, 45, 1897–1899; f) B. Gockel, N. Krause, *Org. Lett.* **2006**, 8, 4485–4492; g) B. D. Sherry, L. Maus, B. N. Laforteza, F. D. Toste, *J. Am. Chem. Soc.* **2006**, 128, 8132–8133; h) N. Morita, N. Krause, *Org. Lett.* **2004**, 6, 4121–4123; i) A. Hoffmann-Röder, N. Krause, *Org. Lett.* **2001**, 3, 2537–2538; j) A. Boutier, C. Kammerer-Pentier, N. Krause, G. Prestat, G. Poli, *Chem. Eur. J.* **2012**, 18, 3840–3844; k) R. E. Kinder, Z. Zhang, R. A. Widenhoefer, *Org. Lett.* **2008**, 10, 3157–3159; l) B. D. Sherry, F. D. Toste, *J. Am. Chem. Soc.* **2004**, 126, 15978–15979; m) N. Morita, N. Krause, *Eur. J. Org. Chem.* **2006**, 4634–4641; n) Z. Zhang, R. A. Widenhoefer, *Org. Lett.* **2008**, 10, 2079–2081; o) J. H. Lee, F. D. Toste, *Angew. Chem.* **2007**, 119, 930–932; *Angew. Chem. Int. Ed.* **2007**, 46, 912–914; p) C. Deutsch, B. Gockel, A. Hoffmann-Röder, N. Krause, *Synlett* **2007**, 1790–1794.
- [8] Z. J. Wang, D. Benitez, E. Tkatchouk, W. A. Goddard, F. D. Toste, *J. Am. Chem. Soc.* **2010**, 132, 13064–13071.
- [9] V. Gandon, G. Lemière, A. Hours, L. Fensterbank, M. Malacria, *Angew. Chem.* **2008**, 120, 7644–7648; *Angew. Chem. Int. Ed.* **2008**, 47, 7534–7538.
- [10] a) K. L. Butler, M. Tragni, R. A. Widenhoefer, *Angew. Chem.* **2012**, 124, 5265–5268; *Angew. Chem. Int. Ed.* **2012**, 51, 5175–5178; b) Z. Zhang, C. F. Bender, R. A. Widenhoefer, *J. Am. Chem. Soc.* **2007**, 129, 14148–14149; c) Y.-M. Wang, C. N. Kuzniewski, V. Rauniyar, C. Hoong, F. D. Toste, *J. Am. Chem. Soc.* **2011**, 133, 12972–12975.
- [11] a) S. Montserrat, G. Ujaque, F. López, J. L. Mascareñas, A. Lledós, *Top. Curr. Chem.* **2011**, 302, 225–248; b) D. Benitez, E. Tkatchouk, A. Z. Gonzalez, W. A. Goddard III, *Org. Lett.* **2009**, 11, 4798–4801; c) B. Trillo, F. López, S. Montserrat, G. Ujaque, L. Castedo, A. Lledós, J. L. Mascareñas, *Chem. Eur. J.* **2009**, 15, 3336–3339; d) M. Malacria, L. Fensterbank, V. Gandon, *Top. Curr. Chem.* **2011**, 302, 157–182; e) I. Fernández, F. P. Cossío, A. de Cázar, A. Lledós, J. L. Mascareñas, *Chem. Eur. J.* **2010**, 16, 12147–12157; f) I. Alonso, B. Trillo, F. López, S. Montserrat, G. Ujaque, L. Castedo, A. Lledós, J. L. Mascareñas, *J. Am. Chem. Soc.* **2009**, 131, 13020–13030.
- [12] a) T. J. Brown, A. Sugie, M. G. D. Leed, R. A. Widenhoefer, *Chem. Eur. J.* **2012**, 18, 6959–6971; b) T. J. Brown, A. Sugie, M. G. Dickens, R. A. Widenhoefer, *Organometallics* **2010**, 29, 4207–4209.
- [13] Plotting  $\ln[\text{ee} (R)\text{-2a}]$  versus time is equivalent to plotting  $\ln\{[(R)\text{-2a}]_t - [(R)\text{-2a}]_\infty\}$  versus time. In all cases, the value  $k_{\text{rac}}$  corresponds to the second-order rate constant for racemization ( $k_{\text{rac}} = k_{\text{obs}}[\text{catalyst}]$ ), which is equal to two times the rate constant for enantiomerization; see ref. [14].
- [14] a) C. Wolf, *Dynamic Stereochemistry of Chiral Compounds: Principles and Applications*, RSC, Cambridge, **2008**; b) A. Cope, K. Banholzer, H. Keller, B. A. Pawson, J. J. Whang, H. J. S. Winkler, *J. Am. Chem. Soc.* **1965**, 87, 3644–3649.
- [15] M. Preisenberger, A. Schier, H. Schmidbaur, *J. Chem. Soc. Dalton Trans.* **1999**, 1645–1650.
- [16] R. E. M. Brooner, T. J. Brown, R. A. Widenhoefer, *Chem. Eur. J.* **2013**, 19, 8276–8284.
- [17] T. J. Brown, M. G. Dickens, R. A. Widenhoefer, *Chem. Commun.* **2009**, 6451–6453.
- [18] a) R. E. M. Brooner, R. A. Widenhoefer, *Angew. Chem.* **2013**, 125, 11930–11941; *Angew. Chem. Int. Ed.* **2013**, 52, 11714–11724; *Angew. Chem.* **2013**, 125, 11930–11941; b) H. Schmidbaur, A. Schier, *Organometallics* **2010**, 29, 2–23; c) M. A. Cinelli, in *Modern Gold Catalyzed Synthesis* (Eds.: A. S. K. Hashmi, D. F. Toste), Wiley-VCH, Weinheim, **2012**, pp. 153–199.
- [19] a) T. J. Brown, R. A. Widenhoefer, *J. Organomet. Chem.* **2011**, 696, 1216–1220; b) R. A. Sanguramath, T. N. Hooper, C. P. Butts, M. Green, J. E. McGrady, C. A. Russell, *Angew. Chem.* **2011**, 123, 7734–7737; *Angew. Chem. Int. Ed.* **2011**, 50, 7592–7595; c) R. A. Sanguramath, S. K. Patra, M. Green, C. A. Russell, *Chem. Commun.* **2012**, 48, 1060–1062; d) R. E. M. Brooner, R. A. Widenhoefer, *Organometallics* **2011**, 30, 3182–3193; e) E. Herrero-Gómez, C. Nieto-Oberhuber, S. López, J. Benet-Buchholz, A. M. Echavarren, *Angew. Chem.* **2006**, 118, 5581–5585; *Angew. Chem. Int. Ed.* **2006**, 45, 5455–5459; *Angew. Chem.* **2006**, 118, 5581–5585; f) P. Pérez-Galán, N. Delpont, E. Herrero-Gómez, F. Maseras, A. M. Echavarren, *Chem. Eur. J.* **2010**, 16, 5324–5332; g) Y. Zhu, C. S. Day, L. Zhang, K. J. Hauser, A. C. Jones, *Chem. Eur. J.* **2013**, 19, 12264–12271; h) Y. Zhu, C. S. Day, A. C. Jones, *Organometallics* **2012**, 31, 7332–7335.
- [20] T. Fueno, T. Okuyama, T. Deguchi, J. Furukawa, *J. Am. Chem. Soc.* **1965**, 87, 170–174.
- [21] H. Kurosawa, N. Asada, *J. Organomet. Chem.* **1981**, 217, 259–266.
- [22] H. Kurosawa, T. Majima, N. Asada, *J. Am. Chem. Soc.* **1980**, 102, 6996–7003.
- [23] K. Ohkita, H. Kurosawa, T. Hirao, I. Ikeda, *J. Organomet. Chem.* **1994**, 470, 189–190.
- [24] a) T. J. Williams, A. D. Kershaw, V. Li, X. Wu, *J. Chem. Educ.* **2011**, 88, 665–669; b) R. L. Jarek, R. J. Flesher, S. K. Shin, *J. Chem. Educ.* **1997**, 74, 978–982; c) L. R. Dalton, *Adv. Magn. Reson.* **1976**, 8, 149–259, d) S. Forsén, R. A. Hoffman, *J. Chem. Phys.* **1963**, 39, 2892–2901; e) S. Forsén, R. A. Hoffman, *Acta Chem. Scand.* **1963**, 17, 1787–1788.
- [25] W. R. Roth, G. Ruf, P. W. Ford, *Chem. Ber.* **1974**, 107, 48–52.
- [26] a) C. S. Drucker, V. G. Toscano, R. G. Weiss, *J. Am. Chem. Soc.* **1973**, 95, 6482–6484; b) O. Rodriguez, H. Morrison, *J. Chem. Soc. Chem. Commun.* **1971**, 679–679.
- [27] A. Claesson, L.-I. Olsson, *J. Chem. Soc. Chem. Commun.* **1979**, 524–525.
- [28] a) A. Horváth, J.-E. Bäckvall, *Chem. Commun.* **2004**, 964–965; b) J. Deska, C. del Pozo Ochoa, J.-E. Bäckvall, *Chem. Eur. J.* **2010**, 16, 4447–4451.
- [29] H. E. Burks, S. Liu, J. P. Morken, *J. Am. Chem. Soc.* **2007**, 129, 8766–8773.
- [30] G. A. Molander, E. M. Sommers, S. R. Baker, *J. Org. Chem.* **2006**, 71, 1563–1568.
- [31] D. N. Tran, N. Cramer, *Angew. Chem.* **2013**, 125, 10824–10828; *Angew. Chem. Int. Ed.* **2013**, 52, 10630–10634.
- [32] J. D. Osborne, H. E. Randell-Sly, G. S. Currie, A. R. Cowley, M. C. Willis, *J. Am. Chem. Soc.* **2008**, 130, 17232–17233.
- [33] S. M. Oon, W. M. Jones, *Organometallics* **1988**, 7, 2172–2177.
- [34] A. C. Cope, W. R. Moore, R. D. Bach, H. J. S. Winkler, *J. Am. Chem. Soc.* **1970**, 92, 1243–1247.
- [35] H. Schlossarczyk, W. Sieber, M. Hesse, H.-J. Hansen, H. Schmid, *Helv. Chim. Acta* **1973**, 56, 875–944.
- [36] Z. K. Sweeney, J. L. Salsman, R. A. Andersen, R. G. Bergman, *Angew. Chem.* **2000**, 112, 2429–2433; *Angew. Chem. Int. Ed.* **2000**, 39, 2339–2343.
- [37] P. v. R. Schleyer, T. M. Su, M. Saunders, J. C. Rosenfeld, *J. Am. Chem. Soc.* **1969**, 91, 5174–5176.
- [38] K. Izawa, T. Okuyama, T. Sakagami, T. Fueno, *J. Am. Chem. Soc.* **1973**, 95, 6752–6756.
- [39] H. Mayr, W. Foerner, P. v. R. Schleyer, *J. Am. Chem. Soc.* **1979**, 101, 6032–6040.
- [40] T. Okuyama, K. Izawa, T. Fueno, *J. Am. Chem. Soc.* **1973**, 95, 6749–6752.
- [41] K. Troshin, H. Mayr, *J. Org. Chem.* **2013**, 78, 2649–2660.
- [42] C. Reichardt, T. Welton, in *Solvents and Solvent Effects in Organic Chemistry*, Wiley-VCH, Weinheim, **2010**.
- [43] a) D. Zuccaccia, L. Belpassi, F. Tarantelli, A. Macchioni, *J. Am. Chem. Soc.* **2009**, 131, 3170–3171; b) D. Zuccaccia, L. Belpassi, L. Rocchigiani, F. Tarantelli, A. Macchioni, *Inorg. Chem.* **2010**, 49, 3080–3082.
- [44] a) K. Vrieze, H. C. Volger, M. Gronert, A. P. Praat, *J. Organomet. Chem.* **1969**, 16, P19–P22; b) K. Vrieze, H. C. Volger, A. P. Praat, *J. Organomet. Chem.* **1970**, 21, 467–475.

- [45] B. Foxman, D. Marten, A. Rosan, S. Raghu, M. Rosenblum, *J. Am. Chem. Soc.* **1977**, *99*, 2160–2165.
- [46] Because the allene moiety of  $\pi$ -4,5-nonadiene complex **1b** has a C-C-C angle of approximately  $165^\circ$ , as determined by X-ray crystallography (see ref. [12]), both of these  $\eta^1$ -allene complexes are presumably bent to some degree.
- [47] R. L. LaLonde, W. E. Brenzovich, Jr., D. Benitez, E. Tkatchouk, K. Kelley, W. A. Goddard III, F. D. Toste, *Chem. Sci.* **2010**, *1*, 226–233.

---

Received: March 22, 2014

Published online on August 8, 2014